

Comparisons of the relative effects of polyhydroxyl compounds on local versus long-range motions in the mitochondrial inner membrane. Fluorescence recovery after photobleaching, fluorescence lifetime, and fluorescence anisotropy studies

Brad Chazotte *

Department of Cell Biology and Anatomy, School of Medicine, University of North Carolina, Chapel Hill, NC 27599-7090, USA

Received 23 February 1994

Abstract

This laboratory has been interested in understanding the relationship between molecular motion and electron transport rates in the mitochondrial inner membrane. We have previously noted a sucrose-induced decrease in both multicomponent electron transport rates and lateral diffusion of redox components. The decreases in lateral diffusion and the related mobile fraction of redox components were greater than expected from hydrodynamic theory. In this report we sought to understand how the presence of increasing aqueous concentrations of polyhydroxyl agents affect short-range motions in different regions of the inner membrane bilayer, frequently expressed in terms of 'viscosity' and order, compared to lateral diffusion. Fluorescence recovery after photobleaching was used to monitor long-range phospholipid and integral protein diffusion. Multifrequency fluorescence lifetime and steady-state fluorescence anisotropy techniques were used to monitor local dynamics of diphenylhexatriene (DPH) and trimethylaminodiphenylhexatriene (TMA-DPH). Light scattering corrections were found to be essential for inner membrane measurements by the latter two techniques. DPH and TMA-DPH each exhibited two-lifetime components. Generally, increasing the aqueous concentration of polyhydroxyl agents decreased the average DPH lifetime and increased the average TMA-DPH lifetime. In general, under the same conditions fluorescence anisotropies increased. Our results indicated that changes in the rotational diffusion coefficient, microviscosity and order were being induced at both the phospholipid headgroup and in the acyl chain regions of the *membrane* bilayer. Our results suggest that these changes may be due in part to induced changes in the interaction and distribution of water with membranes. Long-range lateral diffusion was found to be significantly retarded by increasing concentrations of polyhydroxyl agents. We conclude that the discrepancies between bulk viscosity predicted decreases in long-range diffusion may result, in part, from the aforementioned membrane/water interactions. We also note an apparent qualitative relationship between long-range lateral diffusion reported diffusion coefficient with local TMA-DPH reported rotational diffusion coefficient and apparent microviscosities.

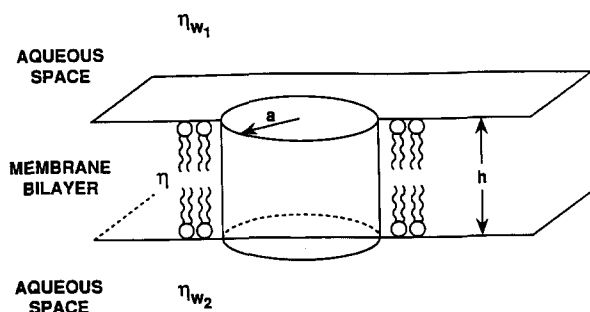
Key words: Bioenergetics; Biomembrane; Diffusion; Sucrose; Glycerol; Membrane dynamics; Hydration

1. Introduction

Our laboratory has been studying the relationship between molecular motion in the mitochondrial inner membrane and electron transport rates within the context of the Random Collision Model of Mitochondrial Electron Transport that we have proposed. This model [1] postulates, in part, that all electron transfers are

Abbreviations: DPH, 1,6-diphenyl-1,3,5-hexatriene; TMA-DPH, 1-[4-(trimethylamino)phenyl]-6-phenylhexa-1,3,5-triene; FRAP, fluorescence recovery after photobleaching; r_s , steady-state anisotropy; D , long-range lateral diffusion coefficient; D_r , rotational diffusion coefficient; Complex III, ubiquinol:cytochrome *c* oxidoreductase; DiI, 3,3'-diethyldecylindocarbocyanine; P, poise; S , order parameter.

* Corresponding author. Fax: +1 (919) 9661856.



SAFFMAN-DELBRÜCK FOR: $\eta_w \ll \eta$ $\eta_{w1} = \eta_{w2}$

$$D_T = \frac{kT}{4\pi\eta h} \left(\ln \frac{\eta h}{\eta_w a} - \gamma \right)$$

$$D_R = \frac{kT}{4\pi a^2 \eta}$$

HUGHES, *et al.* FOR: $\varepsilon \leq 1$ or $\eta_w \leq \eta$

$$D_T = \frac{kT}{4\pi(\eta_{w1} + \eta_{w2})a} \times \varepsilon \left[\ln(2/\varepsilon) - \gamma + 4\varepsilon/\pi - (\varepsilon^2/2) \ln(2/\varepsilon) + O(\varepsilon) \right]$$

$$\text{where } \varepsilon = \frac{(\eta_{w1} + \eta_{w2})a}{\eta h}$$

Fig. 1. The hydrodynamic treatment of Saffman and Delbrück and of Hughes and coworkers for diffusion in membranes. The illustration depicts a schematic representation of a diffusing cylinder in a membrane and the physical parameters involved in the calculations. See text for details.

preceded by one or more diffusion-based collisions. In this context factors that affect lateral diffusion can potentially affect the rates of electron transport. Related to this model, we published a study on the temperature dependence of lateral diffusion and electron transport at different protein densities in the mitochondrial inner membrane from which we concluded that the lateral diffusion of ubiquinone with its redox partners is rate-limiting in the native mitochondrion for maximum rates of electron transport [2].

We sought to employ another classic way of approaching the question of a rate-limiting step whereby the solvent viscosity is increased. As formulated by Saffman and Delbrück [3], and extended by Hughes *et al.* [4], a membrane experiences two viscous environments: the membrane phase and the aqueous phase (Fig. 1). We chose to increase the aqueous viscosity by adding viscous agents like sucrose to the aqueous phase and monitor the effects on redox component lateral diffusion and electron transport. In this regard, we previously found that lateral diffusion (long-range motion) of redox components and electron transport rates exhibited corresponding decreases in response to increases in the aqueous sucrose concentration [5]. Sur-

prisingly, the mobile fractions for both the integral protein and phospholipid decreased, a result not expected from the hydrodynamic analyses of Saffman and Delbrück [3] or of Hughes *et al.* [4] nor from early model membrane studies [6].

In this communication we sought to study how increasing aqueous concentrations of polyhydroxyl (viscous) agents affect long-range¹ lateral diffusion measured by FRAP and apparent viscosity compared to local (short-range) membrane motions. We examined local motions in two different regions of the inner membrane bilayer as reported by anisotropies and rotational diffusion coefficients and also expressed them in terms of, the traditionally used, 'microviscosity' and order. In order to determine D_r , microviscosity and order we used multifrequency fluorescence lifetime and steady-state fluorescence anisotropy techniques with DPH and TMA-DPH probes.

We found that the agents tested do affect the short-range motions in the mitochondrial inner membrane, as frequently described by D_r , microviscosity and order. Qualitatively an increase in one or more of these parameters accompanies decreases in lateral diffusion when the aqueous concentration of the viscous agents tested increased. There appears to be a reasonable correlation between TMA-DPH reported D_r and apparent microviscosity with lateral diffusion. However, we could not establish a simple quantitative or proportional relationship between changes in the long-range lateral diffusion with microviscosity and order, e.g., D or its apparent viscosity with the local D_r or its microviscosity. Nonetheless, our data indicate that changes do occur in the membrane itself as the aqueous environment is altered. Among the possible reasons we offer to explain these results are changes in the membrane hydration and the distribution of water.

2. Methods

2.1. Mitochondrial preparations

Mitochondria were freshly isolated from the livers of male Sprague-Dawley rats using a H300 isolation medium (300 mosM medium comprised of 220 mM mannitol, 70 mM sucrose, 2 mM Hepes, 0.5 mg/ml bovine serum albumin at pH 7.4) according to published protocols [7]. Outer membrane free mitochondria, mitoplasts, were prepared using a controlled digitonin incubation [8]. Mitoplasts were subsequently converted to a simple spherical configuration (called

¹ Long-range diffusion is approximately defined to be in the μm range and short-range diffusion is defined to be ≤ 10 nm as done previously [5].

IMM-40 for inner membrane-matrix) by washing in a hypotonic 40 mosM medium, H40, made as a 7.5-fold dilution of bovine serum albumin-free H300 medium [9].

2.2. Fluorescence recovery after photobleaching

FRAP measurements at 25°C and analyses were carried out as described previously for non-osmotically active, fused, ultralarge mitochondrial inner membranes attached to glass slides [5,10] using a dry 40× objective lens. Immunofluorescence labeling of Complex III, an inner membrane integral redox protein, was carried out as described previously for fused ultralarge inner membranes [5,11] attached to glass microscope slides. Phospholipid diffusion was followed using DiI as previously reported [5], but DiI labeling was done prior to inner membrane fusion. The desired concentration of aqueous agent, e.g., sucrose, was washed through the slide chamber's approximately 40 μ l volume in at least two to three 100 μ l aliquots.

2.3. Fluorescence anisotropy

Steady-state fluorescence anisotropy measurements were determined using a Perkin-Elmer 650–40 spectrofluorometer equipped with an automatic polarization accessory (Woods, Newton, PA). Excitation for DPH was at 355 nm and at 360 nm for TMA-DPH with a 5 nm slit width. Emissions were monitored at 430 nm with a slit width of 10 nm for both probes. All digital intensity readings were signal averaged for 5 s. Readings were made for both labeled and unlabeled inner membranes in the desired medium, e.g., 60% sucrose. A digital thermostated water bath and a separate digital thermometer were used to maintain the cuvette temperature at 25°C. Anisotropy data were recorded and averaged in triplicate using an in-house computer program that also provided error estimates and corrected data for both the instrument G-factor optical correction and the excitation light scattering correction of Shinitsky et al. [12]. Due to the turbid nature of the mitochondrial membrane suspensions data sets were acquired at different membrane concentrations and extrapolated to zero to correct for other potential light scattering artifacts. Fluorescent labeling of inner membranes (2–3 ml) diluted to a concentration of 10 mg/ml was done at 0°C with slow constant stirring adding 1 μ l aliquots of either DPH in tetrahydrofuran or TMA-DPH in EtOH over the course of 1 h to achieve a final probe to lipid ratio of 1:400, a procedure similar to Gupte and Hackenbrock [13]. Control studies to determine residual metabolic function indicated that 95% of succinate oxidase activity could be maintained after labeling by carefully controlling the physical manipulations, e.g., stirring.

2.4. Fluorescence lifetime measurement and analyses

Fluorescence lifetime measurements were carried out on a SLM-48000 multifrequency phase spectrofluorometer. The light source was a 200W Hg-X lamp. A 16 nm entrance slit and a 4 nm exit slit setting for the excitation monochromator was used. Excitation for both DPH and TMA-DPH was at 366 nm. In order to maintain a maximum signal strength a Schott 450 KV filter was used on the emission side in lieu of the monochromator. The polarizer after the Pockel cell was set to 54.7° to eliminate polarization effects. A glycogen solution and a scattering block were used to set the lifetime reference standard at 0 ns. The cuvette temperature was maintained at 25°C using a water bath. Cuvette samples containing 1.0 mg inner membrane protein/ml in the desired medium were constantly stirred during data acquisition. Data were acquired from 10 MHz to 100 MHz every 10 MHz. It was determined that every measurement should be signal-averaged 150 times in order to realize a sufficient signal-to-noise ratio. At each frequency paired sample and reference measurements were taken in duplicate. Thus, on average, each complete data set included 64 000 measurements. Due to the high degree of light scattering (> 5%) for mitochondrial inner membranes and the maximum available excitation signal level, the approach of Rheinhart et al. [14] was required. This necessitated the acquisition of data for unlabeled inner membranes under the exact same conditions as for the labeled and the storage of the AC signal in addition to the normally stored instrument data. The correction for light scattering according to Rheinhart et al. [14] was carried out offline using a spreadsheet macro program originally written by Dr. J. Wu and modified by us. The resultant corrected phase and modulation data frequency file was used subsequently in the lifetime analysis using the Globals Unlimited software. (Preliminary lifetime analysis was done initially using the SLM 48000 software.) Lifetime analyses were done for 1, 2, and 3 components for all data sets and some were tested for the unlikely case of 4 or 5 components on selected data sets. The resultant parameters were the fluorescence lifetime, t_i , SAS_i the fraction of component i (species associated spectra) and χ^2 , a measure of the goodness of the fit of the data. The average lifetime, t_a , was calculated according to Lakowicz [15].

2.5. Calculation of apparent membrane viscosity

The hydrodynamic theory of Saffman and Delbrück [3] has been used for years as a conceptual framework relating diffusion and the resistance to diffusion (viscosity) for the case of biological membranes. This equation, as extended by Hughes et al. [4], was used to derive *apparent* membrane viscosities based on FRAP

long-range lateral diffusion as a function of the bulk aqueous viscosity. Saffman and Delbrück proposed that the lateral diffusion of integral proteins in membranes could be described hydrodynamically as the diffusion of a cylinder in the membrane plane. They stated the following equation for the case of a finite viscosity of the outer liquid (Fig. 1) where, in their equation shown in the figure, k = Boltzman constant, T = temperature in K, h = bilayer thickness, a = diffusant radius, η = the membrane viscosity, η_w = viscosity of the aqueous phase(s) γ = Euler's constant. The Hughes et al. [4] extension (Fig. 1) considers the case where η_w is equal to or somewhat less than the membrane viscosity, a case more appropriate for our studies where we were increasing the aqueous viscosity. Using this approach we calculated apparent membrane viscosities for the mitochondrial inner membrane as defined and accomplished previously [5], but for different aqueous media at 25°C. We also calculated under the same conditions of increased aqueous viscosity predicted D values by holding the inner membrane viscosity invariant at constant temperature. The apparent viscosity was taken as a measure of the hydrodynamic and collisional resistance to motion for the diffusant and is a measure of the physical interaction of the probe with its environment.

2.6. Determination of the membrane order parameter

Anisotropy measurements are comprised of both a dynamic component related to the rate of motion and a

second component related to the range of motion. The order parameter, S , a measure of the range of motion of the phospholipid acyl chains and a component of the membrane 'fluidity' was estimated from steady-state anisotropy measurements using the approach of van der Meer et al. [16]. The equation they derived can be written as $S = r_s / (((r_0 r_s) + (r_0 + r_s)^2) / m)^{0.5}$, where r_s and r_0 equal the steady-state, and limiting anisotropies, respectively, and m is the van der Meer fitting parameter (defined below). For both DPH and TMA-DPH $r_0 = 0.395$. The order parameter can range from zero, totally random, to 1.0, completely ordered.

2.7. Calculation of rotational diffusion coefficient and estimation of membrane microviscosity

The dynamic component of the anisotropy measurement is related to the rotational diffusion motions of a molecule in the membrane and calculation of the D_r depends in part on the fluorescence lifetime of the probe [16–19]. The Perrin equation $r_s = r_0 / (1 + (\tau / \phi))$, where τ = the fluorescence lifetime and ϕ = the rotational correlation time (the latter parameter equals $\eta V / (kT)$), defines the relationship between anisotropy, fluorescence lifetime, and rotational diffusion rigorously for isotropic media. An empirical quantitative relationship was published by van der Meer et al. [16] that corrects the effect of the anisotropic membrane environment on the D_r of the fluorescence probe. The modified equation $6D_r \tau = (r_0 / r_s) - 1 + m$, where the fitting parameter $m = 1.7$ for DPH and 0.6 for TMA-

Table 1
Effect of polyhydroxyl agents on lateral diffusion and membrane hydrodynamics

Medium	$\eta(\text{aq})$ (P)	Relative change	Integral protein					Phospholipid				
			$D(\text{exp})$ ($\times 10^{10}$)	$D(\text{pred})$ ($\times 10^{10}$)	$\eta(\text{mem})$ (P)	relative change	mobile frac.	$D(\text{exp})$ ($\times 10^9$)	$D(\text{pred})$ ($\times 10^9$)	$\eta(\text{mem})$	relative change	mobile frac.
Normal medium	0.01	1	6.9	6.9	88	1	100	3.9	3.9	15.8	1.0	100
10% Sucrose	0.015	1.5	6.9	6.7	85	1	84	2.7	3.8	20.6	1.3	98
30% Sucrose	0.024	2.4	5.0	6.2	113	1.3	31	0.51	3.5	137	8.7	73
60% Sucrose	0.4404	44.04	~ 0	4.0	> 79908	908	0	0.35	2.3	144	9.11	70
20% Glycerol	0.016	1.6	2.8	6.5	230	2.6	40	2.6	3.7	24	1.5	66
40% Glycerol	0.037	3.7	2.1	5.9	298	3.4	29	2.3	3.3	23	1.5	60
60% Glycerol	0.107	10.7	1.0	5.1	592	6.7	14	1.5	2.1	45	2.5	39
10% Sorbitol	0.013	1.3	6.6	4.1	150	1.7	100	1.1	3.8	60	3.8	93
30% Sorbitol	0.029	2.9	6.8	6.0	77	0.9	88	0.78	3.4	83	5.3	83
60% Sorbitol	0.095	9.5	5.1	5.2	119	1.35	80	0.82	2.9	89	5.6	82
15% Fructose	0.015	1.5	6.6	6.5	88	1	72	1.3	3.7	53	3.4	97
31% Fructose	0.028	2.8	1.3	6.1	495	5.6	68	0.98	3.4	65	4.1	89
62% Fructose	0.325	32.5	~ 0	4.2	> 81460	926	0	0.47	2.4	109	6.9	97

Normal medium refers to the H40 isolation medium. Calculations were carried out as described in Methods. The first data column refers to the bulk aqueous viscosity of the solutions at 25°C in Poise and the second column is the change in the viscosity relative to the normal media. $D(\text{exp})$ is the experimental long-range lateral diffusion coefficient determined by FRAP and $D(\text{pred})$ is the lateral diffusion coefficient expected based on the increase in aqueous viscosity in the first column. $\eta(\text{mem})$ is the apparent membrane viscosity required to account for the lower experimental lateral diffusion coefficient. The viscosity for $D = 0$ was calculated based on the highest D that the FRAP instrument would still report as essentially zero.

DPH was used to calculate D_r . The resultant D_r , corrected for the anisotropic membrane environment, was converted to a microviscosity using the standard Perrin equation according to Lakowicz [17]. Comparisons of these fluorescence probe motions to long-range lateral diffusion were then feasible using the resistance to motion, i.e., viscosity, as a quasi-common parameter.

3. Results

3.1. Long-range lateral diffusion and apparent viscosities

The obstructed, long-range lateral diffusion of integral protein and lipoidal molecules in the osmotically inactive, fused, ultralarge mitochondrial inner membranes was progressively retarded by increasing concentrations of viscous agents in the medium (Table 1). However, the experimentally determined D is less than that predicted using the Hughes extension of the Saffman-Delbrück hydrodynamic approach, the bulk aqueous viscosity and the apparent membrane viscosity for the normal membrane. The normal membrane refers to the absence of significant concentrations of polyhydroxyl (viscogenic) agents in the aqueous medium. Only in the case of integral protein diffusion in the presence of sorbitol do experimental and predicted D values match, especially at higher concentrations. These results consider only the mobile fraction of the diffusing components. However, mobile fractions were found to decrease with increasing concentrations of these agents (Table 1). In fact in 60% sucrose or

62% fructose the measured D values were effectively zero, i.e., immobile. Collectively these results indicate that these agents, in addition to their expected viscous effect in the aqueous phase, are indirectly or directly affecting the membrane phase.

3.2. Steady-state anisotropy and membrane order

The steady-state anisotropies exhibited different behaviors depending on the probe and medium (Table 2). First, we consider the anisotropy of DPH which tends to locate in the hydrocarbon region. Sucrose caused the anisotropy of DPH to increase above 10% sucrose in the medium, whereas fructose gave rise to little or no change. Increasing sorbitol in the medium progressively increased DPH anisotropy. Membrane permeant glycerol gave the most dramatic change in anisotropy with an apparent doubling in anisotropy at 20% concentration with a similarly high value at higher concentrations. Control studies with DPH in glycerol/water solutions, i.e., no membranes, yielded anisotropy markedly lower than for the membrane case. Second, we consider TMA-DPH which is located in the phospholipid headgroup region. TMA-DPH exhibited a significant decrease in anisotropy at 10% and 30% sucrose concentration followed by an even more marked increase at 60% sucrose. Fructose exhibited an increase effectively only at its highest, 62% concentration. Glycerol, on the other hand, had a progressive increase in anisotropy with concentration. Sorbitol had a maximum at 30% concentration, but 10% and 60% concentrations were at lower anisotropies for TMA-DPH than in the absence of sorbitol. Changing the composition of the membrane aqueous phase can have significant effects on the membrane phase. However, since the anisotropy has contributions from both order and rotational diffusion and the latter's contribution is affected by the fluorescence lifetime, additional information is required.

The order parameters calculated by the method of van der Meer et al. [16] follow the increases or decreases in the probes' anisotropies (Table 2). The order parameter reported by DPH for the fluid acyl chain region of the membrane bilayer is markedly less than that for headgroup region except for the case of membrane permeant glycerol. For DPH, order appears to increase with increasing concentrations in the aqueous phase except for fructose. Likewise, for TMA-DPH order appears to increase in general, except for sorbitol. Remarkably for glycerol, DPH reports an apparently more ordered environment than for TMA-DPH.

3.3. Determination of the fluorescence lifetimes

Extensive analyses of the data indicated that both DPH and TMA-DPH exhibited two component fluo-

Table 2
Effect of polyhydroxyl agents on steady-state fluorescence anisotropy and the order parameter

Medium	DPH		TMA-DPH	
	r_s	S	r_s	S
Normal medium	0.153	0.497	0.258	0.707
10% Sucrose	0.153	0.497	0.258	0.707
30% Sucrose	0.160	0.517	0.210	0.561
60% Sucrose	0.169	0.543	0.321	0.871
20% Glycerol	0.331	0.907	0.289	0.793
40% Glycerol	0.380	0.980	0.318	0.864
60% Glycerol	0.366	0.961	0.324	0.877
10% Sorbitol	0.155	0.503	0.229	0.620
30% Sorbitol	0.163	0.526	0.275	0.755
60% Sorbitol	0.166	0.535	0.235	0.638
15% Fructose	0.153	0.497	0.255	0.698
31% Fructose	0.150	0.488	0.258	0.707
62% Fructose	0.151	0.491	0.265	0.727

The steady-state anisotropy, r_s , was measured at 25°C and corrected for light scattering; the order parameter, S , was calculated as described in the text. See Methods for details. Normal medium refers to the H40 isolation medium described in Methods.

Table 3
Effect of polyhydroxyl agents on DPH and TMA-DPH fluorescence lifetimes

Medium	Single component			Double component			Triple component									
	<i>t</i>	χ^2	<i>t</i> ₁	SAS ₁	<i>t</i> ₂	SAS ₂	<i>t</i> _a	χ^2	<i>t</i> ₁	SAS ₁	<i>t</i> ₂	SAS ₂	<i>t</i> ₃	SAS ₃	<i>t</i> _a	χ^2
A. probe: DPH																
Normal medium	5.480	16.61	2.705	0.4755	8.377	0.5245	7.093	3.956	2.236	0.300	3.693	0.2661	8.589	0.4339	6.903	4.457
10% Sucrose	4.951	37.04	0.9702	0.5176	6.949	0.4824	6.170	4.424	0.5144	0.300	2.046	0.2755	7.551	0.4245	6.484	4.756
30% Sucrose	4.761	41.87	2.803	0.6812	8.870	0.3188	6.642	30.56	1.402	0.300	7.518	−10 ^{−5}	7.519	0.7000	7.066	80.78
60% Sucrose	5.434	6.415	1.582	0.7618	6.298	0.2381	4.197	2.126	1.574	0.237	6.332	0.300	6.269	0.4625	5.953	2.400
20% Glycerol	4.473	46.91	1.999	0.6497	8.493	0.3503	6.520	11.00	0.5224	0.300	3.005	0.4901	9.883	0.2099	6.752	10.99
40% Glycerol	4.587	25.00	0.916	0.42759	5.959	0.5724	5.439	5.939	0.2357	0.2010	1.272	0.300	6.108	0.4990	5.497	6.617
60% Glycerol	4.379	33.16	1.358	0.4680	6.159	0.5320	5.379	13.89	1.360	0.1670	1.348	0.300	6.150	0.5330	5.375	15.66
10% Sorbitol	5.719	13.25	2.534	0.4391	7.993	0.5609	6.908	2.773	2.130	0.316	5.008	0.300	8.855	0.3841	7.007	2.916
30% Sorbitol	5.587	10.132	2.869	0.4905	8.084	0.5095	6.756	1.097	2.188	0.300	5.729	0.5301	10.58	0.1694	6.890	1.1768
60% Sorbitol	4.836	82.54	2.490	0.6576	9.188	0.3424	6.896	68.71	0.0001	0.0299	1.475	0.6701	4.045	0.300	2.891	22.31
15% Fructose	5.669	7.063	2.800	0.4213	7.622	0.5787	6.604	0.4361	2.453	0.300	4.799	0.2445	8.058	0.4555	6.634	0.4905
31% Fructose	5.831	3.367	3.837	0.5050	7.859	0.4950	6.522	1.049	2.983	0.300	7.020	−1.392	7.007	2.092	6.362	1.301
62% Fructose	5.956	5.610	2.793	0.3575	7.590	0.6425	6.774	0.6219	2.7945	0.300	2.785	0.06	7.589	0.6425	6.769	0.7021
B. probe: TMA-DPH																
Normal medium	2.016	25.71	0.003	0.9929	2.542	0.007	2.194	16.49	−0.8164	0.978	1.853	0.300	1.743	−0.2786	−1.147	17.7
10% Sucrose	2.204	24.86	0.048	0.8936	2.764	0.106	2.418	15.89	0.2356	0.7259	3.322	0.300	7.173	−0.0259	2.058	16.35
30% Sucrose	2.317	22.97	0.0137	0.9658	2.884	0.0342	2.544	19.65	0.0144	0.300	0.0212	0.653	2.884	0.0472	2.547	15.16
60% Sucrose	2.554	14.54	0.0321	0.8722	2.897	0.1277	2.695	12.17	0.5891	0.300	2.777	0.6430	3.850	0.057	2.707	14.63
20% Glycerol	1.919	25.81	0.0003	0.9993	2.382	0.0007	2.062	19.65	0.0977	0.8444	3.175	0.300	3.855	−0.1444	1.855	20.72
40% Glycerol	1.702	61.98	0.0009	0.9982	2.250	0.018	2.202	58.23	0.1250	1.290	0.716	−0.5897	1.2384	0.300	1.609	54.14
60% Glycerol	1.912	29.71	0.0016	0.9950	2.322	0.0050	2.032	25.86	0.1381	1.492	0.5818	−0.7921	1.110	0.300	1.662	11.21
10% Sorbitol	2.614	14.05	0.5368	0.4710	3.229	0.5290	2.882	7.408	0.5330	0.4714	3.220	0.2286	3.233	0.300	2.882	8.362
30% Sorbitol	2.540	5.769	2.087	0.8850	3.657	0.1150	3.017	2.024	2.098	0.5842	2.061	0.300	5.641	0.1158	3.016	2.285
60% Sorbitol	2.464	20.18	1.456	0.6491	3.848	0.3509	2.863	16.24	1.451	0.6465	3.820	0.0535	3.839	0.300	2.861	18.33
15% Fructose	2.611	6.750	1.554	0.5949	3.796	0.4051	2.954	1.996	1.513	0.300	1.593	0.2944	3.794	0.4055	2.954	2.253
31% Fructose	2.724	7.962	1.143	0.4535	3.547	0.5465	3.040	2.256	1.138	0.4526	3.544	0.2477	3.545	0.300	3.039	2.547
62% Fructose	2.791	4.444	1.469	0.4406	3.559	0.559	3.046	1.479	1.135	0.300	2.872	0.5120	4.201	0.1880	3.048	1.686

See text for details.

rescent lifetimes (Table 3). However, TMA-DPH's lifetimes effectively reduce to one component for sucrose and glycerol since the lifetime with the largest fraction is of sub-nanosecond duration. The turbid characteristics and size of the mitochondrial inner membranes gave rise to a significant amount of light scattering which made the data difficult to acquire and quantitate. The use of the method of Rheinhardt et al. [14] to correct for light scattering was essential. A representative plot of the phase and modulation as a function of frequency is shown for the experimental data and the resultant global fit for two component lifetimes for DPH in mitochondrial inner membranes in the presence of 62% fructose (Fig. 2). Four criteria were used to assess the number of lifetime components. The fit that produced the lowest reduced χ^2 derived from the Global Unlimited fitting algorithms was chosen over that with a higher value. Any fits that resulted in physically impossible negative lifetimes or component fractions were disregarded. Any multicomponent fits that produced two lifetimes with almost the same values were considered to be the same lifetime. All fits were examined for consistency for a given agent and among all the agents. Reduced χ^2 values for one component lifetimes were consistently higher than that for two or three components (Table 3) indicating that one component lifetimes were the least favorable choice. The χ^2 for two components were generally less than that for three. In a significant number of instances the three component fit yielded negative lifetimes or component fractions that were clearly impossible (Ta-

ble 3). Also in a number of three component fits only two distinguishably different lifetimes were calculated (Table 3). Higher order, 4 and 5 component fittings did not produce better results (data not shown) and are inherently less reliable due to the greater number of variables. On these bases the results of the two lifetime components were used for subsequent analyses and calculations.

The lifetimes and component fractions of DPH and TMA-DPH were altered by changes in the aqueous medium (Table 3). Despite the fact that a number of researchers have reported two lifetime components for DPH [20,21], the photophysics of DPH and the related TMA-DPH have increasingly been found to be more complicated than originally thought. In fact, the reason for the existence of short component lifetime is not agreed upon. Consequently we have used in our analysis here, as have others, the average lifetime to reflect the complicated changes in individual component lifetimes and their respective fractions in a more tractable way. The average lifetime of DPH was generally found to be shorter in the presence of the added aqueous agents as compare to the normal (H40) medium. The greatest effect was seen at high sucrose or fructose concentrations, whereas sorbitol had the least pronounced effect. The average lifetime of TMA-DPH was found to increase with increasing concentrations of aqueous agents except for glycerol. TMA-DPH exhibited a subnanosecond lifetime component in the normal, sucrose and glycerol media and for sucrose the fraction of this component seemed to decrease relative

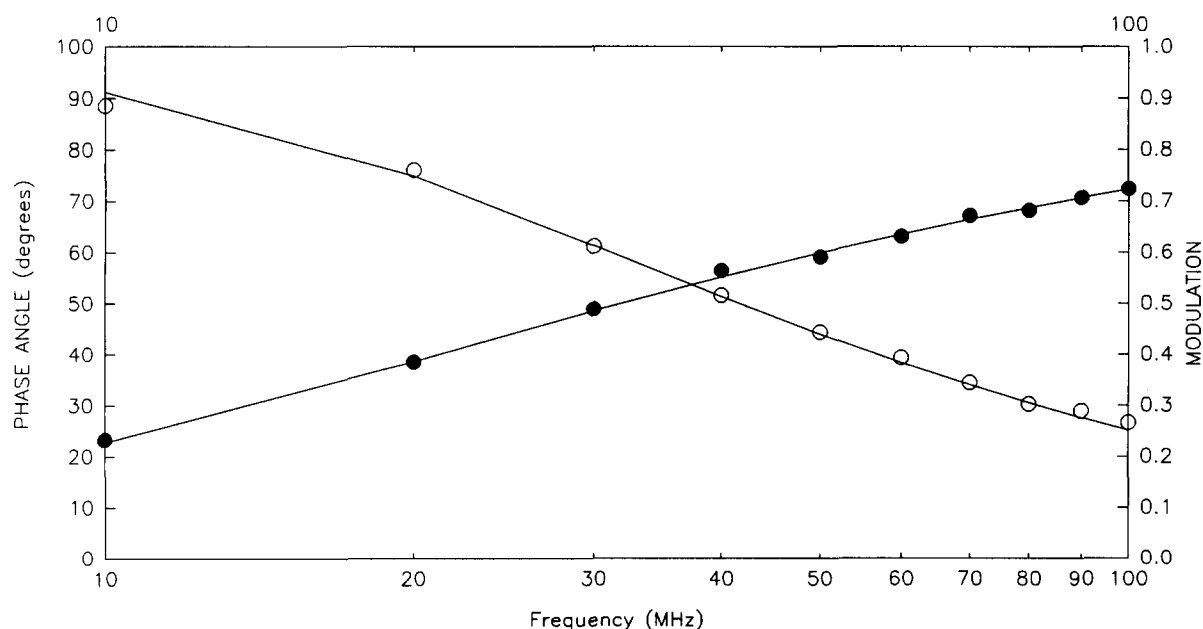


Fig. 2. Representative plot of phase and modulation as a function of frequency for DPH in mitochondrial inner membranes in the presence of 62% fructose. The symbols are for phase raw data (●) and modulation raw data (○). The Global Unlimited fitting procedure was for two component lifetimes and is represented by the solid lines.

to the normal medium. In the presence of sorbitol or fructose the shorter lifetime component was increased into the nanosecond range and was a significantly smaller component fraction.

3.4. Rotational diffusion coefficients and estimation of membrane microviscosities

The DPH-reported D_r increased in the presence of sucrose, decreased dramatically in the presence of glycerol, increased slightly in the presence of fructose, but was relatively unchanged by sorbitol (Table 4). For TMA-DPH the reported D_r increased initially in the presence of sucrose and dramatically decreased in 60% sucrose (Table 4). Fructose engendered a progressive yet significant decrease in the reported D_r and a similar effect is seen with glycerol. Sorbitol gives a greater value than for the normal medium, but the 30% sorbitol value may be aberrantly low compared to 10% and 60% sorbitol concentrations.

The concept of a microviscosity, in terms of a resistance to motion, has traditionally been used in the literature of the last twenty years. We have used this approach to permit a comparison of anisotropy and fluorescence lifetime reported changes to local (probe) motions in the bilayer with the long-range lateral motions detected by FRAP. Unfortunately the current state of theory does not yet permit a more rigorous comparison and any approach entails significant assumptions. This obtains for the hydrodynamic ap-

proach of Saffman-Delbrück [3] and of Hughes et al. [4] for membrane component diffusion, as well as that of van der Meer et al. [16] for utilizing the Perrin equation with fluorescent probes in membranes. Nonetheless, given these caveats our microviscosity results seem reasonable (Table 4).

The DPH- or TMA-DPH- reported microviscosity will change opposite to the D_r (Table 4). Some confidence in the numerical results of this approach derives from the fact that apparent values for the microviscosity (Table 4) are in the accepted range for mitochondrial phospholipids [22–24] using other instrumental techniques and TMA-DPH-reported microviscosities are greater than those reported by DPH. It is clear that the physically different agents studied affect the membrane phase in the acyl chain region, as well as phospholipid headgroup region, in addition to their effects on the aqueous phase.

3.5. Comparison of long-range lateral diffusion and local anisotropy-derived changes

It has been customary in the literature to express the resistance to motion in membranes in terms of viscosity or microviscosities. We have therefore examined the relative effects of increasing the concentration of a given aqueous agent by plotting the membrane properties reported by lateral diffusion and fluorescence probes with that for the aqueous viscosity. (Aqueous viscosity and the FRAP-derived, apparent

TABLE 4

Effect of polyhydroxyl agents on short-range membrane dynamics measured by fluorescence anisotropy and fluorescence lifetime

Medium	DPH				TMA-DPH			
	μ (P)	relative change in μ	D_r $\times 10^{-7}$	ϕ (s) $\times 10^9$	μ (P)	relative change in μ	D_r $\times 10^{-7}$	ϕ (s) $\times 10^9$
Normal medium	0.554	1.0	7.71	2.16	0.885	1.0	8.59	1.94
10% Sucrose	0.482	0.870	8.86	1.88	0.767	0.867	9.91	1.18
30% Sucrose	0.520	0.938	8.22	2.03	0.784	0.886	9.70	1.72
60% Sucrose	0.354	0.639	12.1	1.38	1.48	1.67	5.14	3.25
20% Glycerol	0.883	1.59	4.84	3.44	0.973	1.10	7.81	2.13
40% Glycerol	0.802	1.45	5.33	3.13	1.19	1.35	6.37	2.62
60% Glycerol	0.775	1.40	5.51	3.02	1.13	1.28	6.72	2.49
10% Sorbitol	0.545	0.983	7.84	2.13	0.992	1.12	7.66	2.18
30% Sorbitol	0.555	1.0	7.71	2.16	1.33	1.50	5.72	2.91
60% Sorbitol	0.574	1.04	7.44	2.24	1.02	1.15	7.46	2.24
15% Fructose	0.516	0.931	8.28	2.01	1.17	1.33	6.48	2.57
31% Fructose	0.502	0.905	8.52	1.96	1.23	1.39	6.20	2.69
62% Fructose	0.524	0.945	8.16	2.04	1.27	1.44	5.97	2.79

Apparent microviscosity calculations at 25°C of the corrected D_r with the Perrin equation employed a value of $C(r) = 860\,000$, a parameter incorporating the equivalent spherical volume of a fluorophore, for DPH based on Lakowicz [17]. For TMA-DPH a value of $C(r) = 1\,530\,000$ was calculated, as had been done for DPH, using Eq. [14] of Shinitsky and Barenholz [47] using the data in Figs. 3A and 9 of Prendergast et al. [35] and Fig. 1 of Lentz et al. [48]. The relative change in μ compares the apparent microviscosity relative to the normal (H40 isolation) medium. D_r in this table is corrected for the anisotropic membrane environment according to van der Meer et al. [16]. Likewise ϕ is the corrected rotational correlation time. See Methods.

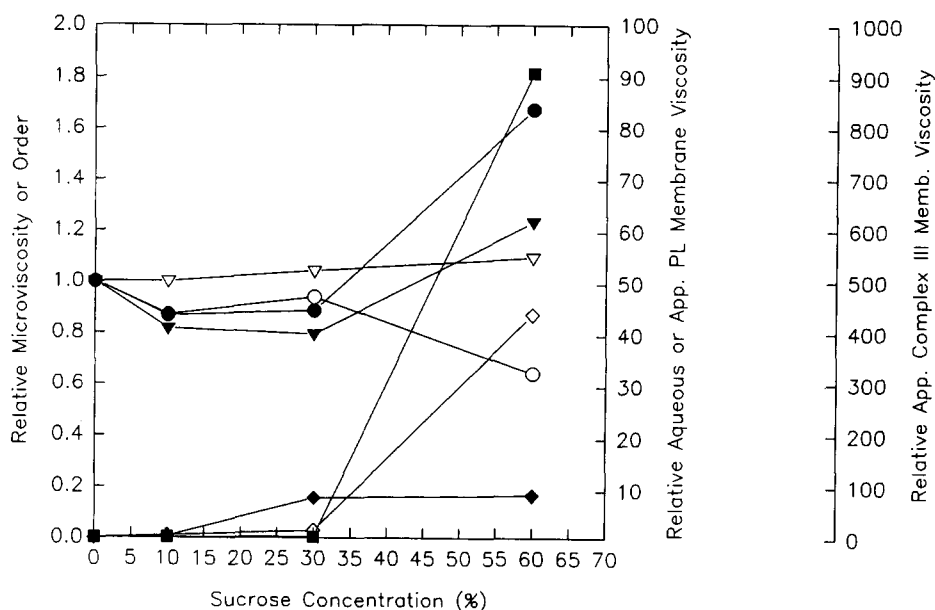


Fig. 3. Relative changes in viscosities and order parameters for mitochondrial inner membrane as a function of sucrose concentration (w/v). The bulk aqueous viscosity (◇) and the phospholipid, lateral diffusion-based apparent membrane viscosity (◆) are plotted relative to the near right y-axis. The Complex III, lateral diffusion-based, apparent membrane viscosity (■) is plotted relative to the far right y-axis. The DPH (○) and TMA-DPH (●) reported microviscosities and the DPH (▽) and TMA-DPH (▼) reported order parameters are plotted against the left y-axis. Values were calculated as stated in Methods as normalized to their respective values for normal mitochondrial inner membranes, i.e., in H40 isolation medium. All parameters are for 25°C.

membrane viscosity are plotted on the right y-axis and the DPH and TMA-DPH derived apparent microviscosity are plotted on the left y-axis.) For the case of sucrose the most pronounced increases in the apparent membrane viscosity and TMA-DPH reported microviscosity and order occur at concentrations greater than 30% which mirrors the large increase in aqueous vis-

cosity (Fig. 3). DPH-reported microviscosity tends to decrease whereas the reported order parameter progressively increases (Fig. 3). The same type of plot for glycerol (Fig. 4) shows a similar increase in apparent membrane viscosity and aqueous viscosity which is more pronounced at higher glycerol concentrations. Likewise there is an increase in the TMA-DPH reported micro-

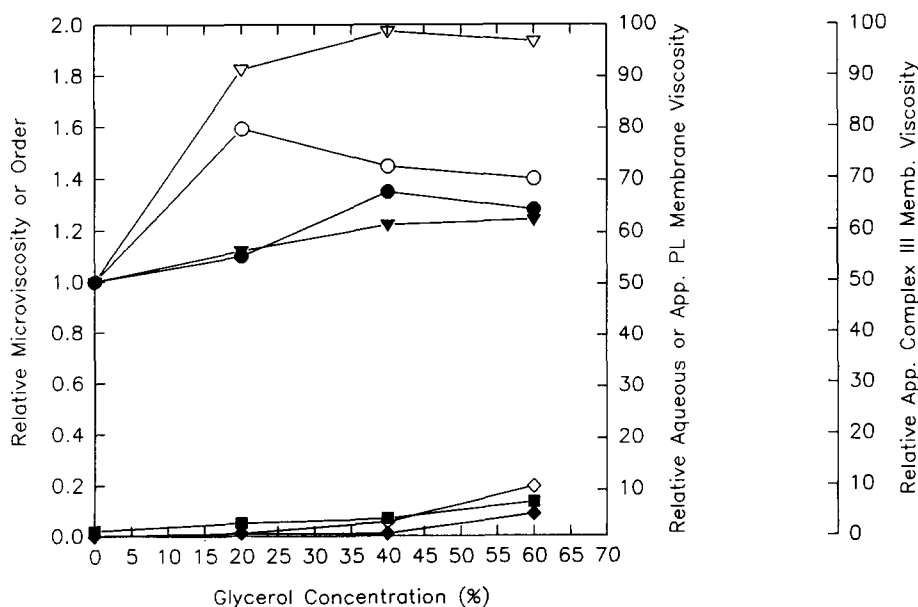


Fig. 4. Relative changes in viscosities and order parameters for mitochondrial inner membrane as a function of glycerol concentration. Details as in the legend for Fig. 3.

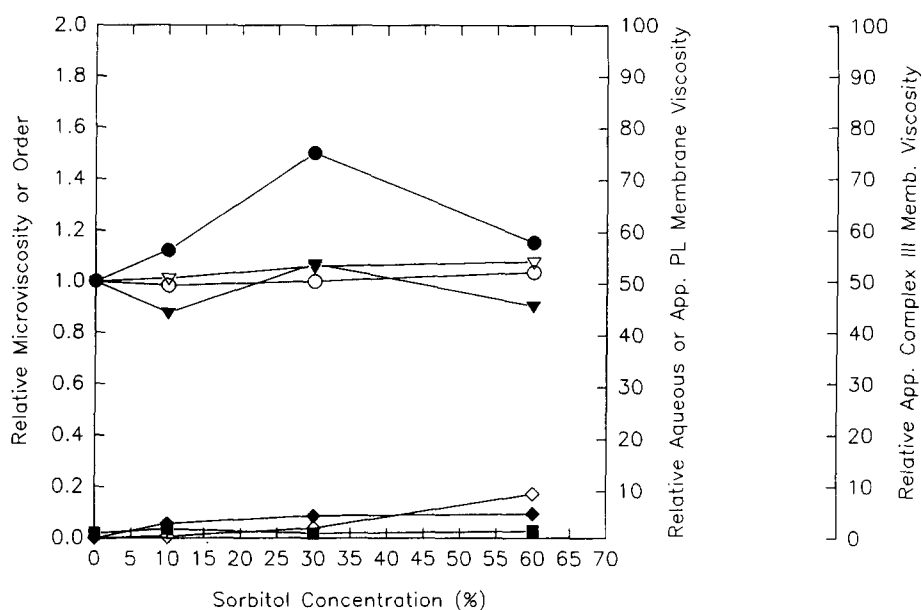


Fig. 5. Relative changes in viscosities and order parameters for mitochondrial inner membrane as a function of sorbitol concentration. Details as in the legend for Fig. 3.

viscosity, but in contrast to sucrose, a steady progressive increase in the order parameter (Fig. 4). On the other hand, the DPH-reported phenomena increased dramatically starting at the lowest glycerol concentration with less dramatic changes with increasing concentration. Sorbitol induced an increase in the apparent membrane viscosity with increasing concentration, and, except for the increase in TMA-DPH microviscosity, little change was seen in order or DPH-reported microviscosity (Fig. 5). Fructose produced a progressive

increase in the apparent membrane viscosity reported by phospholipid, whereas that reported by Complex III increased dramatically above a concentration of 31% similar to sucrose (Fig. 6). Little change in DPH-reported order and a slight decrease in microviscosity were observed. TMA-DPH, in contrast, reported a marked increase in microviscosity starting at a 15% concentration which continued to increase thereafter. TMA-DPH reported order exhibited little apparent change. While DPH- and TMA-DPH-reported micro-

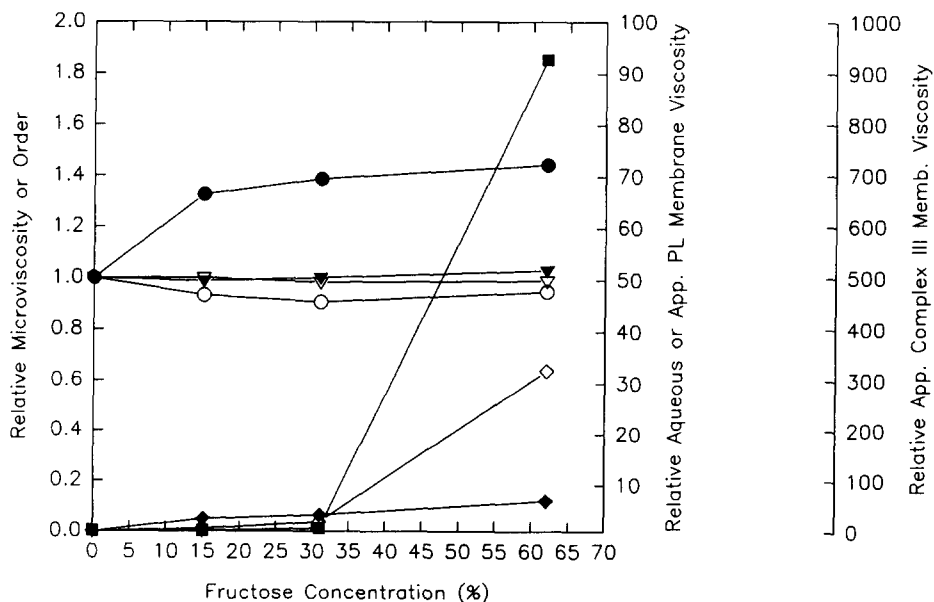


Fig. 6. Relative changes in viscosities and order parameters for mitochondrial inner membrane as a function of fructose concentration. Details as in the legend for Fig. 3.

viscosity and order may or may not independently report effects on the apparent membrane viscosity, generally it qualitatively appears that TMA-DPH-reported microviscosity increases when this long-range-diffusion reported viscosity is increased by increasing concentration of aqueous agents.

4. Discussion

4.1. Hydrodynamic analysis of lateral diffusion

Our results showed that for both integral protein and membrane lipids D values (and mobile fractions) decreased by increasing aqueous concentrations of the viscous (polyhydroxyl) agents. The fact that phospholipids were affected as well as the integral proteins that project more extensively than lipids into the aqueous phase, suggests that the effect is not solely dependent on the extent of contact with the aqueous phase. Since the membranes used in the lateral diffusion measurements were not osmotically active the effects cannot be attributed to a bulk osmotic effect across the mitochondrial inner membrane, typically observed as shrinking and swelling of a vesicle.

The decrease in long-range, lateral diffusion we found may well reflect changes induced in the interaction and distribution of water molecules with the membrane. This redistribution can be thought of in terms of an osmotic effect on the membrane. Related to our diffusion studies, NMR measurements of diffusion in phospholipid multibilayers found that diffusion decreased as the membrane hydration was decreased [25]. Similarly, McCown et al. [26] reported that the D for NBD-phosphatidylethanolamine decreased as the degree of hydration of egg phosphatidylcholine decreased. Stumpel et al. [27] reported that increasing sucrose concentration alters the X-ray diffraction pattern and calorimetric behavior of phospholipid multibilayers in a manner consistent with the dehydration of the membrane. A comparison of these reports with our analyses of our fluorescence lifetime and anisotropy data below further supports this hypothesis.

The results we report showed that the Saffman-Delbrück hydrodynamic approach overestimates the lateral diffusion coefficient in mitochondrial inner membranes as the aqueous concentration of the viscous agent is increased. A similar overestimate has been reported by Vaz et al. [28] following NBD-MSPE, a lipid analogue, diffusion in 1-palmitoyl-2-oleoylphosphatidylcholine model membranes in the presence of 60–70% sucrose. Both these reports are in apparent contrast to the portion of the published report of Peters and Cherry [6] using reconstituted bacteriorhodopsin containing bilayers which found an excellent agreement between experiment and theory as the

sucrose concentration was increased from 0 to 48% at 32°C. Our results, those of Peters and Cherry [6] and Vaz et al. [28] disagree with the report of Ollmann et al. [29] that found little effect for the aqueous phase on membrane diffusion monitored by excimer formation.

It is our conjecture that the Saffman-Delbrück hydrodynamic approach runs into difficulty on the assumption that the two phases (membrane and aqueous) are independent. At high concentrations of these polyhydroxyl agents, the agents exert physical effects (e.g., osmotic) on the *membrane phase*, possibly altering the membrane's viscosity. In most cases this occurs at fairly high concentrations not normally encountered in vivo and not typical for most in vitro experiments. At high concentrations even the Hughes et al. [4] extension, intended for cases where the aqueous viscosity is close to that of the membrane, does not sufficiently compensate. Since both protein and lipid diffusion are affected the extent of the discrepancy in D between theory and experiment cannot be solely attributed to the extent the diffusant projects into the aqueous phase. Our results should not be construed to invalidate the basic concept of Saffman-Delbrück approach, rather it highlights the need for additional refinements in more complex cases. One possible refinement might consider that the viscosity of the membrane/aqueous interface is more strongly affected than the bulk aqueous or membrane viscosities utilized in the Saffman-Delbrück approach.

It is not altogether clear from our data how one would explain the significant increases in the immobile fractions of both protein and lipoidal lateral diffusants. The changes in anisotropy-reported microviscosity or order generally are relatively small and do not explain large increases in immobile fractions, and attempts at plotting relative or absolute changes in order parameter, anisotropy or immobile fraction with one another did not reveal any clear relationships (data not shown). It is possible that these polyhydroxyl agents are introducing microdomain formation which could have a more significant effect on long-range diffusion as opposed to local dynamics. Microdomain formation is suggested by the ability of some sugar alcohols and disaccharides to introduce hexagonal phase into membranes at high concentrations [30]. A multidomain membrane would have a significant affect on long-range lateral diffusion (see for example Almeida et al. [31]) The effect would be similar to that of increasing the integral membrane protein concentration, which is known to retard lateral diffusion [5]. In such an environment DPH and TMA-DPH fluorescent probes could be in microdomains. (It is known that DPH does not preferentially partition in, e.g., gel versus liquid phase.) Despite the normally low probe to phospholipid ratio used, the presence of DPH or TMA-DPH in a microdomain might have an enhanced effect as an impu-

rity, resulting in a probe-induced fluidization of the local environment [18], thus preventing greater actual changes from being reported.

4.2. Fluorescence lifetimes in mitochondrial inner membranes

Our finding of two fluorescent lifetime components for DPH and our roughly 7–8 ns and 2–3 ns lifetime ranges are consistent with a number of other reports in the literature [20,21,32–34]. We are not aware of any published studies concerning the mitochondrial inner membrane used in our studies. Alternatively, analysis of DPH using a lifetime distribution analysis generally results in lifetimes centered around two ‘peaks’ (e.g., Fiorini et al. [32]) in lieu of a double exponential decay. No definitive judgment has been made in the literature concerning one approach over the other, nor is there agreement on the photophysical nature of the shorter lifetime component of DPH.

Our TMA-DPH data are in agreement with literature reports of a shorter lifetime (2–3 ns) compared to DPH in membranes [35]. The cited study made only single frequency measurements which would not reveal two lifetime components. The existence of two lifetime components for TMA-DPH is suggested by our results for inner membranes in the presence of sorbitol and fructose and by analogy to its parent molecule DPH with which TMA-DPH shares a number of photophysical properties. For our normal H40 medium and in glycerol the average lifetime reflects the longer-lived component although it comprises a small fraction of the fluorophore population and this lifetime effectively appears to be single component. The physical meaning of the very short lifetime is more difficult to establish, perhaps it could reflect a quenching of TMA-DPH, since fluorescence quenching reduces the observed lifetime [36].

Clearly our data show that there are changes induced in the fluorescence lifetimes of both DPH and TMA-DPH on the basis of component lifetimes and their fractional distribution or on the basis of the average lifetime which includes both of the former parameters. These changes must be considered in the interpretation of steady-state anisotropy studies of membrane dynamics. Our observed changes in fluorescence lifetime may well reflect changes in membrane lipid packing and/or water penetration of the membrane bilayer [37,38]. Greater penetration of water into the bilayer is thought to be favored by discontinuities in phospholipid acyl residues’ van der Waals interactions [38]. The presence of water gives rise to changes in the interior bilayer polarity (dielectric constant) which the probe experiences. Increasing the dielectric constant decreases the fluorescence lifetime [34,37]. Thus, the general tendency for the average lifetime of

TMA-DPH to increase with increasing concentrations may well reflect a decrease in the hydration in the headgroup region of the bilayer monitored by the probe. For DPH, the general tendency for the average lifetime to decrease under the same conditions may reflect increased water penetration into the bilayer interior. Clearly water distribution at the bilayer surface and membrane interior is being affected by the agents used in our study.

4.3. Aqueous phase effects on steady-state anisotropy measurements of mitochondrial inner membranes

The alterations in anisotropy induced by increasing the aqueous concentrations of polyhydroxyl agents are consistent with the literature. Sucrose was found to increase the anisotropy of horse bean root and 1,2-dioleoyl-*sn*-3-phospho-*rac*-(1-glycerol) phospholipid vesicles with a more marked increase above 30% sucrose, while 1,2-dioleoyl-*sn*-3-phosphocholine was relatively unaffected below 30% sucrose [39]. This study concluded that sucrose alters the polar headgroup solvation perhaps affecting hydrogen bonding [39]. Relatedly and in general agreement with our findings, deuterium NMR studies of the interaction of polyhydroxyl agents with model lipid membranes have revealed that these agents induce concentration dependent changes in phospholipid (phosphatidylcholine) headgroups [40]. We reported that different agents had different regional, i.e., DPH versus TMA-DPH, effects. Others [40] found that in the membrane’s hydrophobic interior one agent could induce a small ordering effect, while another could induce disordering there and in the headgroup region. This was related to the ability of polyhydroxyl agents to change water’s structure and associations [40]. The importance of water on order and rotational diffusion in membranes is further supported by an EPR study on oriented multibilayers where a nitroxide spin label anchored in the phospholipid headgroup region, analogous to TMA-DPH, reported decreases in order and increases in mobility correlated with increases in water content [41].

We can only hypothesize as to the reason for the anomalous approximate 2-fold increase in DPH anisotropy in the presence of glycerol. Glycerol, the only membrane permeant agent used in this study, may well intercalate with the hydrocarbon chains causing the large increase. (Glycerol at high concentrations is known to profoundly affect membrane structure introducing interdigitated phases in model membranes.) Since up to 80% glycerol/water solutions did not yield anisotropies as high we concluded that the observed change was not due to a solubilization of the DPH molecule in the aqueous phase and out of the membrane. Similarly, since anisotropy for DPH was markedly higher than for TMA-DPH at the same gly-

erol concentration, we did not ascribe the change reported by DPH to movement to the headgroup region of the bilayer where TMA-DPH normally resides.

4.4. Possible relationships between long-range lateral diffusion and local fluorescence polarization

Our results indicate that there is some relationship between fluorescence polarization and lateral diffusion in biological membranes in that decreases in fluorescence anisotropy-derived D_r , i.e., local increases in resistance to motion (viscosity), and/or order may be reflected in decreases in long-range lateral diffusion. This is, however, a qualitative relationship and the TMA-DPH probe located in the headgroup region may report on this relationship. Thus, our report is not necessarily in conflict with the data in the much earlier report of Kleinfeld et al. [42]. They reported a lack of a relationship between DPH-reported anisotropies and lateral diffusion in lymphocyte plasma membranes treated with different concentrations of free fatty acids to induce fluidity changes in the membrane phase. Our approach focused on changes in the aqueous phase using polyhydroxyl agents to alter the bulk aqueous phase viscosity. In addition to our use of both TMA-DPH and DPH, their report did not consider the possibility of microdomains on lateral diffusion and/or fluorescence anisotropy, nor induced changes in probe fluorescence lifetimes which affect the interpretation of the local probe motion.

Questions may be raised as to whether the region of the membrane bilayer reported by DPH or that reported by TMA-DPH separately and/or independently can affect the lateral diffusion reported by FRAP. Both integral proteins and phospholipids have a portion of their mass in both of these regions. Is the most 'viscous' region of the membrane the determining factor for lateral diffusion or is it some combination of the two? Theory is not yet at the point of adequately addressing such issues. Also the relationship of short-range motion and order on long-range diffusion is not well understood. It seems unlikely that the two are 'decoupled'. It can be conjectured that if a molecule such as a phospholipid is to move it must have a space to move into, i.e., free volume, and if it is difficult to move in a local regime then it should be more difficult to create a free volume for a diffusant to move into and that this could have a significant effect on the repetitions necessary to move long-range.

While a qualitative relationship between the resistance to long-range lateral diffusion and the short-range D_r , (local) microviscosity and/or order parameter of TMA-DPH or DPH may be made, a simple quantitative relationship does not currently appear possible, nor is theory adequate. The apparent viscosity reported by long-range lateral diffusion (in essence, the long-

range lateral diffusion coefficient itself) includes both the influence, to some extent, of the local microviscosity and the effect of multicollisional, obstructed, long-range diffusion (cf. Chazotte and Hackenbrock [5]). Thus, the apparent viscosity based on lateral diffusion is much higher than the DPH-based microviscosity. Our data also shows that a simple comparison of the relative increase or decrease in long-range versus local viscosity is not tractable.

4.5. Interactions of polyhydroxyl agents with membranes

There are a number of published studies in the literature examining how polyhydroxyl compounds like sucrose interact with hydrated and dehydrated membranes [43,44]. Some of this interest was rooted in the membrane stabilizing effect of these agents during dehydration and freezing [44,45]. It has been noted that the agents used in this study strongly interact with water and have also been shown to increase the thermal stability of protein and may raise the phase transition temperature of phospholipid membranes [44,46]. An underlying theme in these studies appears to be how these polyhydroxyl agents affect the distribution and interaction of water with respect to membranes. Our studies also suggest a significant role for water, but in modulating the dynamic motions in membranes. We conclude that decreases in lateral diffusion in mitochondrial inner membranes induced by polyhydroxyl agents like sucrose exert both an aqueous phase viscous effect and alter the structure and distribution of water at or in the membrane, thus, giving rise to larger effects than from bulk viscosity alone.

Acknowledgements

The author would like to thank Dr. Barry Lentz, in particular, for the generous use of the fluorescence lifetime instrument, for helpful discussions, and for suggesting the light scattering correction approach of Rheinhart et al. [14]; Dr. B. Wieb van der Meer for a critical review of the manuscript; Dr. K.A. Jacobson, for extensive discussions; Dr. C.R. Hackenbrock for his encouragement and support; Dr. Jogen Wu for help in my use of the fluorescence lifetime instrument and related software; Drs. X.F. Wang, J. Lakowicz and J. Eisinger for helpful discussions; Mike Sports and Ian Heath for mitochondrial preparations. Supported in part by NSF 88-16611 and NIH GM28704.

References

- [1] Hackenbrock, C.R., Chazotte, B. and Gupte, S.S. (1986) *J. Bioenerg. Biomembr.* 18, 331–368.

- [2] Chazotte, B. and Hackenbrock, C.R. (1989) *J. Biol. Chem.* 264, 4978–4985.
- [3] Saffman, P.G. and Delbrück, M. (1975) *Proc. Natl. Acad. Sci. USA* 72, 3111–3113.
- [4] Hughes, B.D., Pailthorpe, B.A., White, L.R. and Sawyer, T. (1982) *Biophys. J.* 37, 673–676.
- [5] Chazotte, B. and Hackenbrock, C.R. (1988) *J. Biol. Chem.* 263, 14359–14367.
- [6] Peters, R., and Cherry, R.J. (1982) *Proc. Natl. Acad. Sci. USA* 79, 4317–4321.
- [7] Schneider, H., Lemasters, J.J., Höchli, M. and Hackenbrock, C.R. (1980) *Proc. Natl. Acad. Sci. USA* 77, 442–446.
- [8] Schnaitman, C. and Greenawalt, J.W. (1968) *J. Cell Biol.* 38, 158–175.
- [9] Hackenbrock, C.R. (1972) *J. Cell Biol.* 53, 450–465.
- [10] Hackenbrock, C.R. and Chazotte, B. (1986) *Methods Enzymol.* 125, 35–45.
- [11] Chazotte, B. and Hackenbrock, C.R. (1991) *J. Biol. Chem.* 266, 5973–5979.
- [12] Shinitzky, M., Dianoux, A.-C., Gitler, C. and Weber, G. (1971) *Biochemistry* 10, 2106–2113.
- [13] Gupte, S.S. and Hackenbrock, C.R. (1988) *J. Biol. Chem.* 263, 5241–5247.
- [14] Rheinhart, G.D., Marazola, P., Jameson, D.M. and Gratton, E. (1991) *J. Fluoresc.* 1, 153–162.
- [15] Lakowicz, J.R. (1983) *Fluorescence Spectroscopy*, pp. 51–91, Plenum Press, New York, NY.
- [16] Van der Meer, B.W., Van Hoeven, B. and Van Blitterswijk, W. (1986) *Biochim. Biophys. Acta* 854, 38–44.
- [17] Lakowicz, J.R. (1981) in *Spectroscopy in Biochemistry* (Bell, J.E., ed.), Vol. 1, pp. 195–244, CRC Press, Boca Raton, FL.
- [18] Lentz, B.R. (1988) in *Spectroscopic Membrane Probes*, (Lowe, L., ed.), Vol. 1, pp. 13–41, CRC Press, Boca Raton, FL.
- [19] Stubbs, C.D. and Williams, B.W. (1992) in *Topics in Fluorescence Spectroscopy* (Lakowicz, J.R., ed.), Vol.3, pp. 231–272, Plenum Press, New York, NY.
- [20] Barrow, D.A. and Lentz, B.R. (1985) *Biophys. J.* 48, 221–234.
- [21] Parasassi, T., De Stasio, G., Rusch, R.M. and Gratton, E. (1991) *Biophys. J.* 59, 466–475.
- [22] Keith, A., Blufield, G. and Snipes, W. (1970) *Biophys. J.* 10, 618–629.
- [23] Keough, K.M., Oldfield, E., Chapman, D. and Benyon, P. (1973) *Chem. Phys. Lipids* 10, 37–50.
- [24] Feinstein, M.B., Fernandez, S.M. and Sha'afi, R.I. (1975) *Biochim. Biophys. Acta* 413, 354–370.
- [25] Kuo, A.L. and Wade, C.G., (1979) *Biochemistry* 18, 2300–2308.
- [26] McCown, J.T., Evans, E., Diehl, S. and Wiles, H.C. (1981) *Biochemistry* 20, 3134–3138.
- [27] Stumpel, J., Vaz, W.L.C. and Hallmann, D. (1985) *Biochim. Biophys. Acta* 821, 165–168.
- [28] Vaz, W.L.C., Stümpel, J., Hallmann, D., Gambacorta, A. and De Rosa, M. (1987) *Eur. Biophys. J.* 15, 111–115.
- [29] Ollmann, M., Robitzki, A., Schwarzmann, G. and Galla, H.J. (1988) *Eur. Biophys. J.* 16, 109–112.
- [30] Bryszewska, M. and Epand, R.M. (1988) *Biochim. Biophys. Acta* 943, 485–492.
- [31] Almeida, P.F.F., Vaz, W.L.C. and Thompson, T.E. (1992) *Biochemistry* 31, 7198–7210.
- [32] Fiorini, R.M., Valentino, M., Glaser, M., Gratton, E. and Curatola, G. (1988) *Biochim. Biophys. Acta* 939, 485–492.
- [33] Williams, B.W. and Stubbs, C.D. (1988) *Biochemistry* 27, 7994–7999.
- [34] Ho, C. and Stubbs, C.D. (1992) *Biophys. J.* 63, 897–902.
- [35] Prendergast, F.G., Haugland, R.P. and Callahan, P.J. (1981) *Biochemistry* 20, 7333–7338.
- [36] Lakowicz, J.R. and Hogen, D. (1980) *Chem. Phys. Lipids* 26, 1–40.
- [37] Zannoni, C., Arcioni, A. and Cavatorta, P. (1983) *Chem. Phys. Lipids* 32, 179–250.
- [38] Parasassi, T., Ravagnan, G., Sapor, O. and Gratton, E. (1992) *Int. J. Radiat. Biol.* 61, 791–796.
- [39] Uso, T. and Rossignol, M. (1984) *FEBS Lett.* 167, 69–72.
- [40] Bechinger, B., Macdonald, P.M. and Seelig, J. (1988) *Biochim. Biophys. Acta* 943, 381–385.
- [41] Korstanje, L.J., Van Fassen, E.E. and Levine, Y.K. (1989) *Biochim. Biophys. Acta* 980, 225–233.
- [42] Kleinfeld, A.M., Dragsten, P., Klausner, R.D., Pjura, W.J. and Matayoshi, E.D. (1981) *Biochim. Biophys. Acta* 649, 471–480.
- [43] Strauss, G., Schurtenberger, P. and Hauser, H. (1986) *Biochim. Biophys. Acta* 858, 169–180.
- [44] Crowe, J.H., Crowe, L.M., Carpenter, J.F., Rudolph, A.S., Wistrom, C.A., Spargo, B.J. and Anchordoguy, T.J. (1988) *Biochim. Biophys. Acta* 947, 367–384.
- [45] Anchordoguy, T.J., Rudolph, A.S., Carpenter, J.F. and Crowe, J.H. (1987) *Cryobiology* 24, 324–331.
- [46] Crowe, L.M., Mouradian, R., Crowe, J.H., Jackson, S.A. and Womersley, C. (1984) *Biochim. Biophys. Acta* 769, 141–150.
- [47] Shinitzky, M. and Barenholz, Y. (1978) *Biochim. Biophys. Acta* 515, 367–394.
- [48] Lentz, B.R., Barenholz, Y. and Thompson, T.E. (1976) *Biochemistry* 15, 4521–4528.